

Reflectivities of Uniform and Broken Marine Stratiform Clouds

James A. Coakley, Jr.

National Center for Atmospheric Research
Boulder, CO 80307

1. Introduction

Plane-parallel radiative transfer models are often used to estimate the effects of clouds on the earth's energy budget and to retrieve cloud properties from satellite observations. Here an attempt is made to assess the performance of such models by using $(1 \text{ km})^2$ AVHRR data collected during the FIRE Marine Stratus IFO to determine the reflectivities and, in particular, the anisotropy of the reflected radiances for the clouds observed during the field experiment. The intent is to determine the anisotropy for conditions that are overcast and to compare this anisotropy with that produced by the same cloud when broken. The observations will thus be used to quantify aspects of the differences between reflection by plane-parallel clouds and non-planar clouds expected on the basis of theoretical studies (McKee and Cox, 1974; Davies, 1978; Welch and Wielicki, 1984 and others).

The results reported are from the 10 daytime passes analyzed during the field experiment (Coakley and Beckner, 1988). These passes coincided with major aircraft missions. The IFO provided a large sample of overcast conditions as is illustrated in Figure 1. The figure shows the frequency of cloud cover occurrence for all of the $(60 \text{ km})^2$ subregions included in the $(500 \text{ km})^2$ regions typically analyzed for each overpass. The predominant condition was overcast. Furthermore, the IFO presented a narrow range of sun-earth-satellite viewing geometries as is illustrated in Figure 2. The figure shows the scattering angle, which is the angle between the direction of the incident sunlight and the reflected radiation observed at the satellite, as a function of the AVHRR scan position. For the IFO radiation undergoes a smoothly varying transition in scattering geometry as a function of the AVHRR scan spot number. At small scan spot numbers radiation is invariably backscattered; at large scan spot numbers it is invariably forward scattered. Reflectivities are reported as a function of AVHRR scan spot position for both uniform and broken clouds and for $0.63 \mu\text{m}$, where scattering is nearly conservative, and $3.7 \mu\text{m}$ where liquid water is moderately absorbing.

2. Data Analysis

To study the properties of uniform clouds and their broken counterparts, cases must be selected for which there is considerable confidence that the cloud is single-layered and either recognizably overcast or clearly broken. The results of the spatial coherence analysis of the AVHRR data are screened following procedures described by Coakley and Davies (1986) to ensure these condition. Furthermore, to ensure that the properties are reported for the same clouds, and to ensure that the properties are representative of the clouds, observations are restricted to $(60 \text{ km})^2$ subframes containing a single cloud layer, and having at least 20% of the area completely overcast while at the same time having at least 20% covered by broken cloud from the same layer. To obtain reflectivities representative

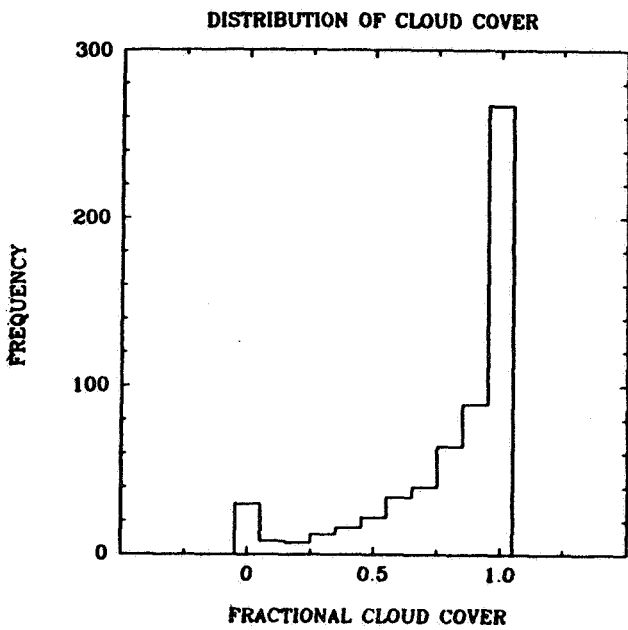


Figure 1. Frequency of cloud cover occurrence for $(60 \text{ km})^2$ subregions derived from the daytime NOAA overpasses analyzed during the FIRE Marine Stratus IFO.

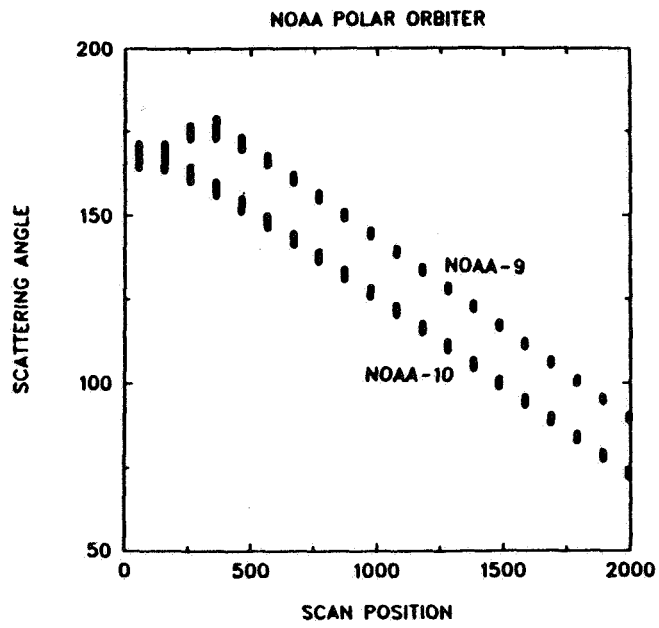


Figure 2. Scattering angle as function of AVHRR scan position for the IFO region and period.

of the broken cloud, allowance is made, to first order, for the fractional cloud cover, which is obtained by the spatial coherence method. That is, the reflectivity associated with broken clouds, r_C , is given by

$$r_C = \frac{r - (1 - A_C)}{A_C} \quad (1)$$

where r is the reflectivity for the portion of the $(60 \text{ km})^2$ subframe for which the fields of view are partially cloud covered and A_C is the fractional cloud cover for these fields of view.

3. Results

Figure 3 shows $0.63 \mu\text{m}$ reflectivities for overcast (open circles-solid line) and broken cloud conditions (dots-dashed line). It is immediately obvious that broken clouds reflect less radiation per unit cloud fraction than do overcast clouds. The decrease is approximately 12% of the overcast reflectivity. This reduction in reflectivity can also be deduced from visible-infrared scatter diagrams. The reduction could be due to either smaller optical depths for the broken clouds or to the effects of cloud geometry (Schmetz, 1984).

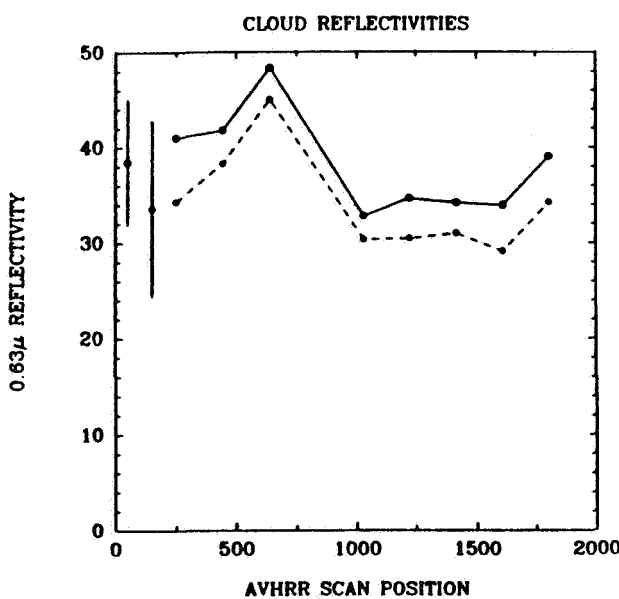


Figure 3. $0.63 \mu\text{m}$ reflectivities as a function of scan position for overcast (open circles-solid line) and broken clouds (dots-dashed line). Observations for both overcast and broken clouds were taken from the same $(60 \text{ km})^2$ subregions. The two data points at the left side of the figure give the mean of all the points and the typical variability of the data points for each recorded scan position.

There is considerable scatter in the reflectivities reported for the various scan positions as is indicated by the error bars in Figure 3. With such variability it is difficult to deduce a trend in the anisotropy. Nevertheless, if a trend exists (that is, the observations are not an idiosyncrasy of the AVHRR or the sparse sample of data), it is for higher reflectivities at forward and backward scattering angles and lower reflectivities at intermediate angles or near nadir viewing. There is no discernible difference in the anisotropy of the radiance fields for overcast and broken clouds.

At $3.7 \mu\text{m}$ liquid water becomes a moderate absorber. The single scattering albedo for marine stratus cloud droplets is approximately 0.9. Figure 4 shows the reflectivities for $3.7 \mu\text{m}$ radiation. To obtain the reflectivities, estimates of emission at $3.7 \mu\text{m}$ were removed from the observed radiances (Coakley and Davies, 1986). As with the visible reflectivities, the reflectivities at $3.7 \mu\text{m}$ show considerable scatter. If there is a trend, it is for higher reflectivities at forward and backward scattering angles and lower reflectivities at intermediate scattering angles. Unlike the visible reflectivities, the reflectivities at $3.7 \mu\text{m}$ for broken clouds are comparable in magnitude, if not greater than those for overcast conditions. The comparable magnitudes is a result of the absorption. With the absorption, the clouds become optically thick at $3.7 \mu\text{m}$ and the resulting reflected radiation is thus unaffected by optical depth or leakage of radiation through the cloud boundaries. Coakley and Davies (1986) also note that the enhancement of reflectivities for broken clouds may

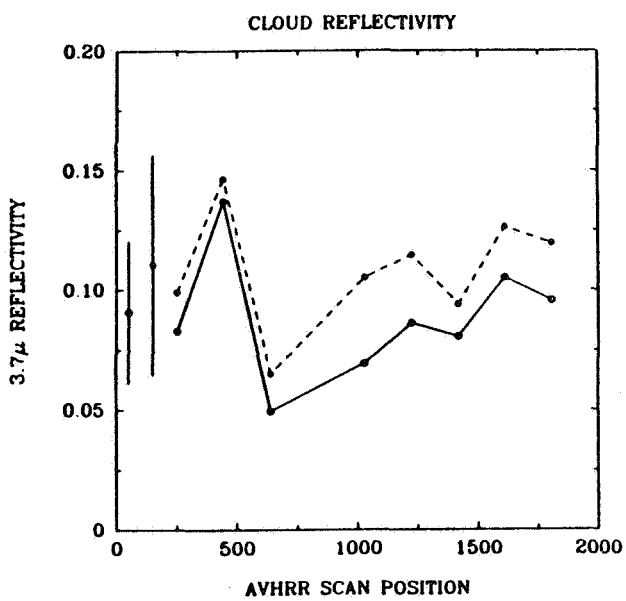


Figure 4. Same as Fig. 3 but for $3.7 \mu\text{m}$.

be due to a systematic shift in cloud droplet size to smaller droplets at cloud edges or to the increased frequency of sun-cloud surface-satellite viewing geometries yielding high reflectivities for the broken clouds.

4. Summary and Conclusions

Reflectivities at visible wavelengths for broken clouds are 88% of the reflectivities of the same clouds under overcast conditions. The decrease in reflectivity for broken clouds may be due to smaller optical depths or to cloud geometrical effects. There is no discernible difference in the anisotropy of the reflectivities between broken and overcast cloud conditions. At $3.7 \mu\text{m}$ where liquid water is a moderate absorber, the reflectivities of broken clouds are comparable to and even greater than those observed for overcast conditions. The lack of a difference at this wavelength is attributed to the amount of absorption, but may also be due to enhancements in the reflectivities for broken clouds that result from the microphysical structure of the cloud and the effects of cloud geometry on reflected radiation.

When data received from PCDS for the IFO period is processed, the results will be added to those presented here. It is anticipated that the increased number of data points will clarify the anisotropy of the reflected radiation and will reveal any differences in the anisotropy for broken and overcast cloud conditions. To remove concerns about a scan dependent response to the AVHRR sensor, correlations of AVHRR reflectivities to those obtained with the ERBE scanner will be made when the ERBE data becomes available. Finally, calculations will be made using plane-parallel cloud models to determine the extent to which such models predict the observed anisotropy for conservative and nonconservative scattering.

Acknowledgement

This work was supported in part by AFGL and AFOSR through transfer of funds to NASA, GLH6-6031 and by NASA Grant L-79877B.

References

Coakley, J.A., Jr. and M.H. Beckner, 1988: Spatial coherence retrievals of cloud properties for the FIRE Marine Stratocumulus IFO, June 29 - July 19, 1987. NCAR/TN-307+STR, 205 pp.

Coakley, J. A., Jr., and R. Davies, 1986: The effect of cloud sides on reflected solar radiation as deduced from satellite observations, *J. Atmos. Sci.*, **43**, 1025-1035.

Davies, R., 1978: The effect of finite geometry on the three-dimensional transfer of solar irradiance in clouds. *J. Atmos. Sci.*, **35**, 1712-1725.

McKee, T.B. and S.K. Cox, 1974: Scattering of visible radiation by finite clouds, *J. Atmos. Sci.*, **31**, 1885-1892.

Schmetz, J., 1984: On the parameterization of the radiative properties of broken clouds, *Tellus*, **36A**, 417-432.

Welch, R.M. and B.A. Wielicki 1984: Stratocumulus cloud field reflected fluxes: The effect of cloud shape. *J. Atmos. Sci.*, **41**, 3085-3103.